CASE 58

Optimization of an Electrical Connector Insulator Contact Housing

Abstract: A computer simulation was used to optimize an electrical connector product design and associated plastic injection molding process. Taguchi's parameter optimization method, in conjunction with finite-element computer simulation, was used to eliminate the need to fabricate expensive tooling and molded parts, leading to faster, more robust product/process designs.

To function correctly the electrical connector must be flat and free of dimensional distortion, to allow reliable insertion of a credit card and proper electrical connection to the embedded computer chip. Three approaches were studied and compared to determine which provides the best set of product/process design parameter values. Smaller-the-better *Z*-axis deflection, dynamic *Z*-axis position, and dynamic mold dimension versus part dimension approaches were compared with respect to the resulting part flatness (*Z*-axis deflection).

1. Introduction

A new generation of CCM02 electrical connectors has been developed within Cannon for use with Smart Cards, a credit card with an embedded computer chip capable of direct communication with a host computer. The connector insulator part (Figure 1) is produced using plastic injection molding technology. For the connector to function reliably, the insulator part needs to be exceptionally flat for surface mounting, allowing the Smart Card to be inserted and interfaced electrically with the contacts mounted in the insulator.

This study presents a comparison between three approaches based on Taguchi's parameter design methods used to optimize the electrical connector product and associated plastic injection molding process. The three approaches were studied and compared to determine which provides the best set of product/process design parameter values. Smaller-the-better *Z*-axis deflection, dynamic *Z*-axis position, and dynamic mold dimension versus part dimension approaches were compared. A computer simulation was used to eliminate the need to fabricate expensive tooling and molded parts. Figure 2 shows the finite-element analysis node mesh used in the computer simulation, which modeled the geometrical position and stress of each node after molding the part.

2. Objective

The objective of the robust engineering effort was to select the best product and process parameter value set which maximizes the function of the injection molding process and results in electrical connector parts that are flat and distortion free. The goal of the study was to explore different robust engineering approaches [i.e., signal-to-noise (SN) ratios] to determine which one resulted in the best product/process parameter configuration.

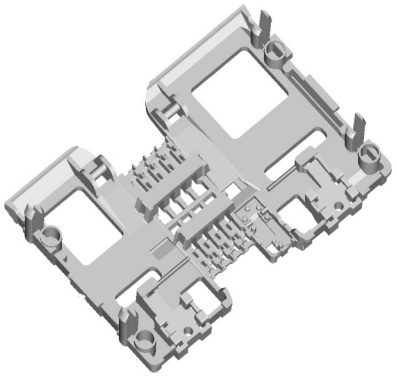

Figure 1
CCM02 MKII electrical connector insulator part

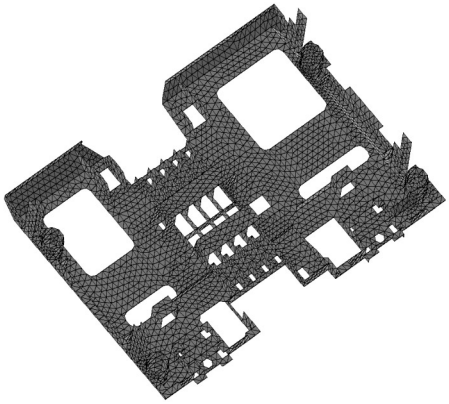

Figure 2
FEA mesh

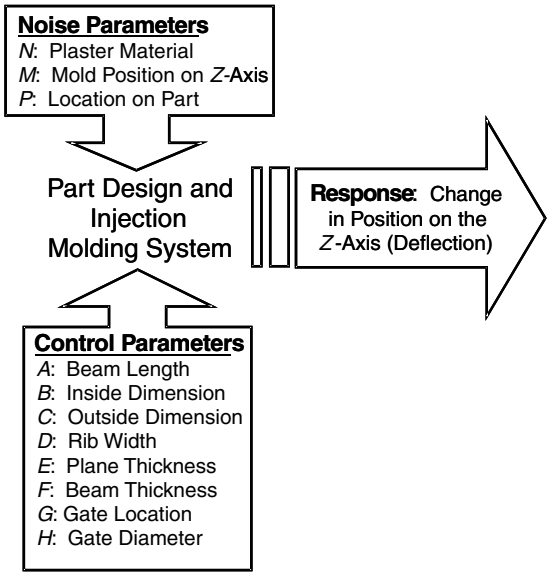

Figure 3
P-diagram for the smaller-the-best approach

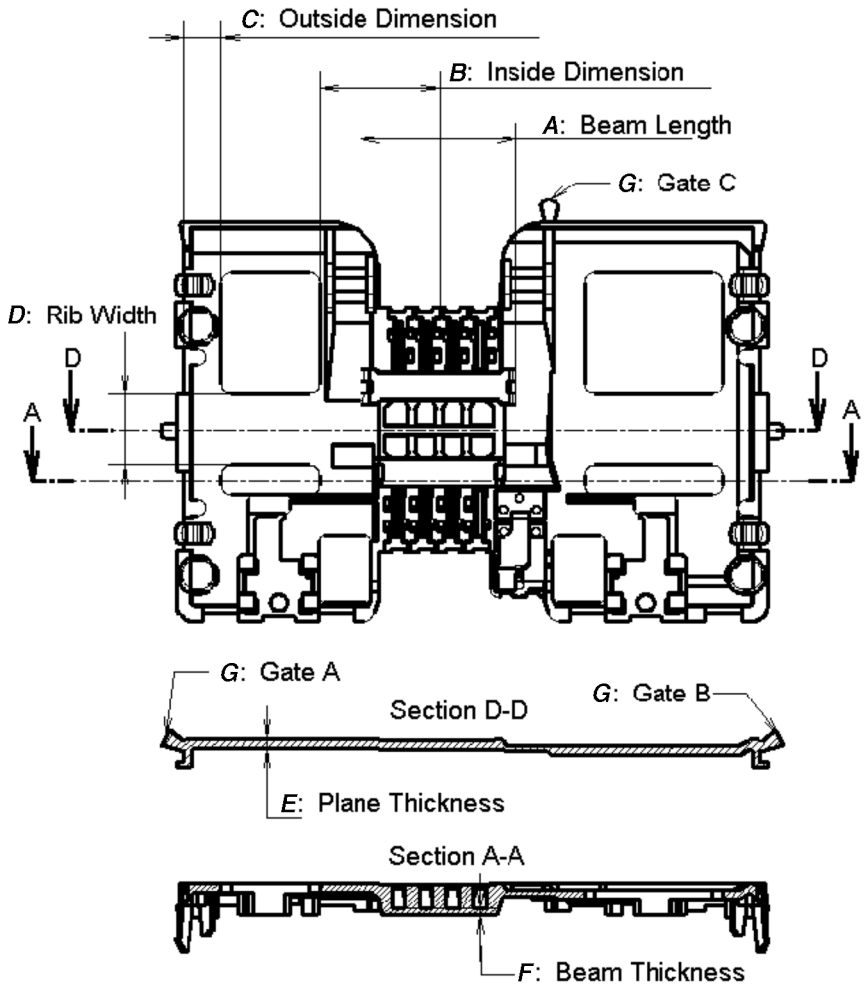

Figure 4
Electrical connector insulator and factor labels

3. Approach 1: Smaller-the-Best Deflection on the *Z*-Axis

After brainstorming the system and comparing past analyses on injection-molded parts of previous versions, the parameter diagram shown in Figure 3 was developed. The static system response was dimensional change along the *Z*-axis from a reference plane parallel to the flat plane of the part. This plane would be analogous to the part lying flat on a table surface with the *Z*-axis perpendicular to the table top. The objective of this approach was to find the best set of product/process design parameter values that results in the smallest amount of dimensional change along the *Z*-axis, zero being the ideal value.

Figure 4 shows the control factors associated with the part design and process parameters. These parameters remain the same for the three approaches discussed in this document. The control parameter

Table 1
Factor levels for the smaller-the-best approach

Factor	Level 1	2	3	4	5	6	7	8	9	10	11	12
Control factors												
A: beam length (mm)	10	12										
B: inside dimension (mm)	11.3	13.6	15.9									
C: outside dimension (mm)	3.38	5.68	7.98									
D: rib width (mm)	0	7	14									
E: plane thickness (mm)	0.6	0.88	1.25									
F: beam thickness (mm)	0.6	0.88	1.25									
G: gate location	*A*	*B*	*C*									
H: gate diameter (mm)	0.4	0.8	1.2									
Noise factors												
N: plastic material	*A*	*B*										
M: *Z*-axis mold position (mm)	0.44	1.04	1.34	1.64	1.96	2.23	2.63	3.04	3.38			
P: location on part (node no.)	1	2	3	4	5	6	7	8	9	11	11	12

values used in an $L_{18}(2 \times 3^7)$ orthogonal array to explore the parameter value design space are presented in Table 1. The noise parameter values, also shown in Table 1, were exposed to the L_{18} using a full-factorial layout.

Table 2 presents the L_{18} orthogonal array with the column assignments used in this computer-simulated parameter optimization study. In addition, the smaller-the-best SN ratios calculated from each row of the data are shown. The raw data values are not presented, due to the large amount of numbers generated for this layout.

This experimental layout was used for all three of the approaches discussed in this document. Figure 5 presents the control-factor-level average graphs for approach 1: smaller-the-best, indicating that the optimum set of control parameter values is $A_1B_1C_2D_3E_3F_2G_1H_2$. Confirmation studies were conducted with this set of control parameter values as well as those of the other two optimization approaches. These are presented later.

4. Approach 2: Dynamic Zero-Point Proportional *Z*-Axis Mold Position versus Part Position

This alternative approach's objective was to select the optimum set of control parameter values that

Table 2
Orthogonal layout for the control factors

OA Row	Control Factor								Smaller-the-Best SN (dB)
	A	*B*	*C*	*D*	*E*	*F*	*G*	*H*	
1	1	1	1	1	1	1	1	1	10.30
2	1	1	2	2	2	2	2	2	14.24
3	1	1	3	3	3	3	3	3	15.27
4	1	2	1	1	2	2	3	3	9.54
5	1	2	2	2	3	3	1	1	15.43
6	1	2	3	3	1	1	2	2	9.49
7	1	3	1	2	1	3	2	3	9.01
8	1	3	2	3	2	1	3	1	12.04
9	1	3	3	1	3	2	1	2	17.75
10	2	1	1	3	3	2	2	1	17.08
11	2	1	2	1	1	3	3	2	8.84
12	2	1	3	2	2	1	1	3	12.03
13	2	2	1	2	3	1	3	2	13.38
14	2	2	2	3	1	2	1	3	10.30
15	2	2	3	1	2	3	2	1	12.53
16	2	3	1	3	2	3	1	2	13.94
17	2	3	2	1	3	1	2	3	17.30
18	2	3	3	2	1	2	3	1	7.50

maximizes the correlation between the signal factor *Z*-Axis mold position and the system's response *Z*-axis part position. The metric selected was the zero-point proportional dynamic SN ratio, and the goal was to select control parameter values levels that maximize this SN ratio and result in a slope as close to 1.00 as possible. This would result in a system that produces a part exactly the shape and size of the mold. The parameter diagram for this approach is shown in Figure 6. Figure 7 shows the ideal function associated with this P-diagram.

Table 3 presents the control, noise, and signal factor levels used in this approach. To accommodate the noise factor location on the Part, 12 locations were selected whose mesh nodes contained the same nine *Z*-axis coordinates used as signal factor values. In this approach, the noise factor *Z*-axis mold position of the smaller-the-best approach became the signal factor for the zero-point proportional dynamic approach.

Figure 8 shows the electrical insulator part finite-element node mesh, indicating the positions used for the noise factor location on the part. Table 4 presents the orthogonal layout used, along with the resulting zero-point proportional SN ratio and slope, β.

Figure 9 shows the control-factor-level average graphs for the zero-point proportional SN ratio for the *Z*-axis position approach, using the values shown in Table 4. Figure 10 presents the sensitivity or slope-factor-level average graphs for the data values shown in Table 4, β.

From these graphs, the best set of control parameter values is $A_1B_1C_2D_3E_3F_2G_1H_2$. Confirmation stud-

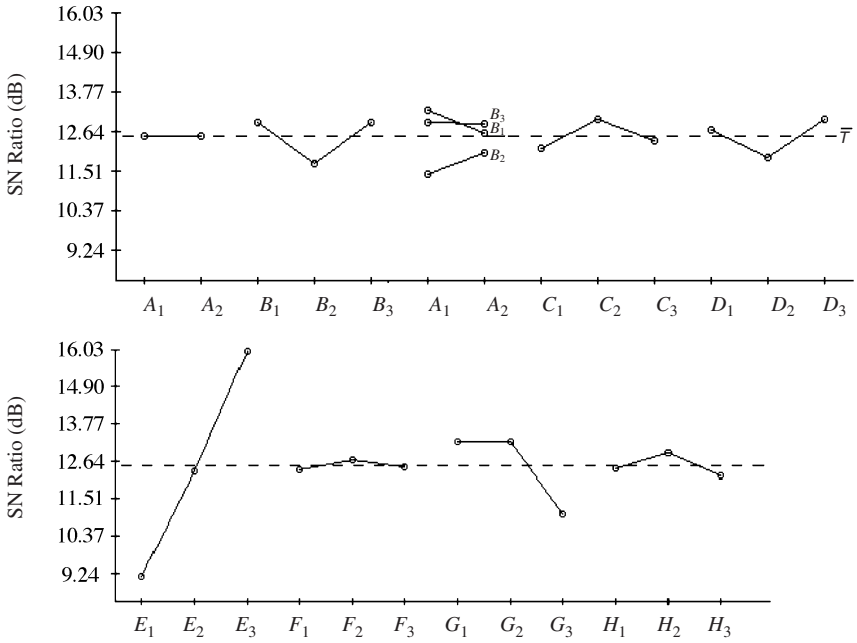

Figure 5
Smaller-the-best control-factor-level average graphs

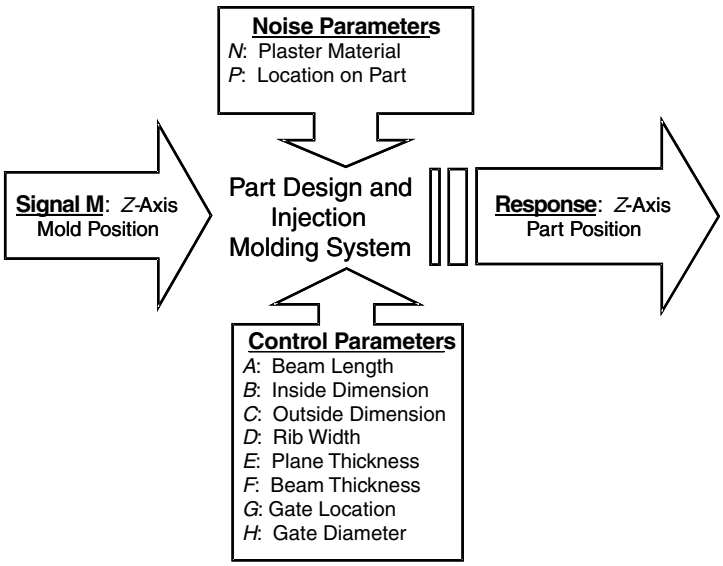

Figure 6
P-diagram for the dynamic *Z*-axis position approach

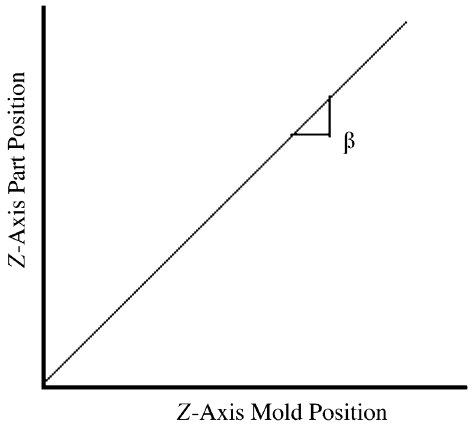

Figure 7
Ideal function for the *Z*-axis position approach

ies were conducted on this set of control factor levels, the results of which are presented along with the other approaches later.

5. Approach 3: Dynamic Zero-Point Proportional Mold Dimension versus Part Dimension, All Axes

The objective of this approach was to select the optimum set of control parameter values that maximizes the correlation between the signal factor, mold dimension, and the system's response, part dimension, using all part axes rather than just the *Z*-axis of approach 2.

Table 3
Factors levels for the *Z*-axis position approach

Factor	Level 1	2	3	4	5	6	7	8	9	10	11	12
Control factors												
A: beam length (mm)	10	12										
B: inside dimension (mm)	11.3	13.6	15.9									
C: outside dimension (mm)	3.38	5.68	7.98									
D: rib width (mm)	0	7	14									
E: plane thickness (mm)	0.6	0.88	1.25									
F: beam thickness (mm)	0.6	0.88	1.25									
G: gate location	*A*	*B*	*C*									
H: gate diameter (mm)	0.4	0.8	1.2									
Noise factors												
N: plastic material	*A*	*B*										
P: location on part (node no.)	1	2	3	4	5	6	7	8	9	11	11	12
Signal factor												
M: *Z*-axis mold position (mm)	0.44	1.04	1.34	1.64	1.96	2.23	2.63	3.04	3.38			

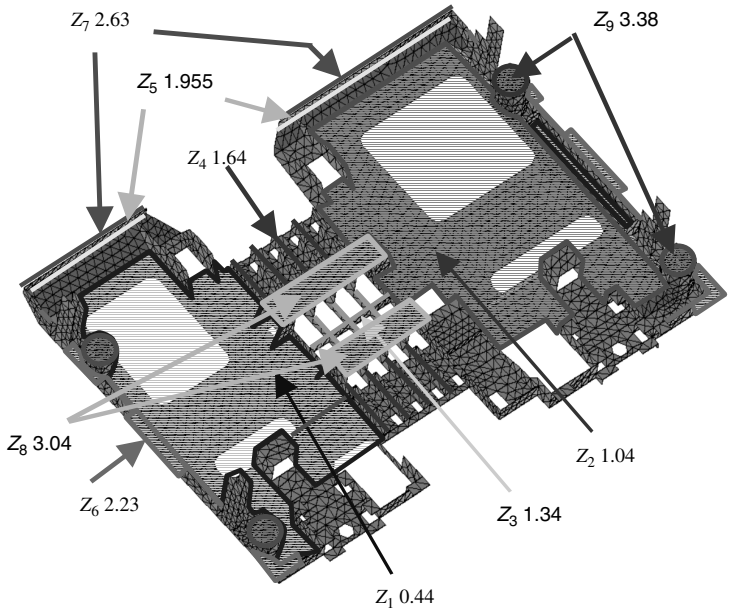

Figure 8
Finite-element node mesh for the *Z*-axis position approach

Table 4
Orthogonal layout and results for the *Z*-axis position approach

OA Row	Control Factor								Zero-Point SN	Slope, β
	A	*B*	*C*	*D*	*E*	*F*	*G*	*H*		
1	1	1	1	1	1	1	1	1	10.22	0.969
2	1	1	2	2	2	2	2	2	14.24	0.981
3	1	1	3	3	3	3	3	3	15.22	0.990
4	1	2	1	1	2	2	3	3	9.43	0.967
5	1	2	2	2	3	3	1	1	15.44	0.984
6	1	2	3	3	1	1	2	2	9.36	0.969
7	1	3	1	2	1	3	2	3	8.89	0.961
8	1	3	2	3	2	1	3	1	11.96	0.983
9	1	3	3	1	3	2	1	2	17.87	0.985
10	2	1	1	3	3	2	2	1	17.12	0.986
11	2	1	2	1	1	3	3	2	8.69	0.970
12	2	1	3	2	2	1	1	3	11.97	0.978
13	2	2	1	2	3	1	3	2	13.35	0.982
14	2	2	2	3	1	2	1	3	10.22	0.969
15	2	2	3	1	2	3	2	1	12.49	0.978
16	2	3	1	3	2	3	1	2	13.98	0.977
17	2	3	2	1	3	1	2	3	17.42	0.984
18	2	3	3	2	1	2	3	1	7.32	0.971

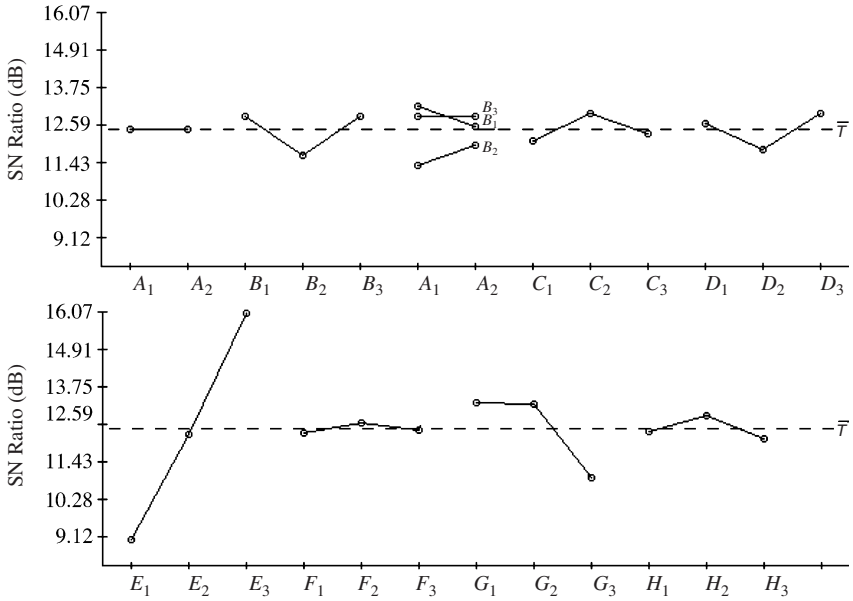

Figure 9
Control-factor-level average graphs for zero-point proportional SN ratio

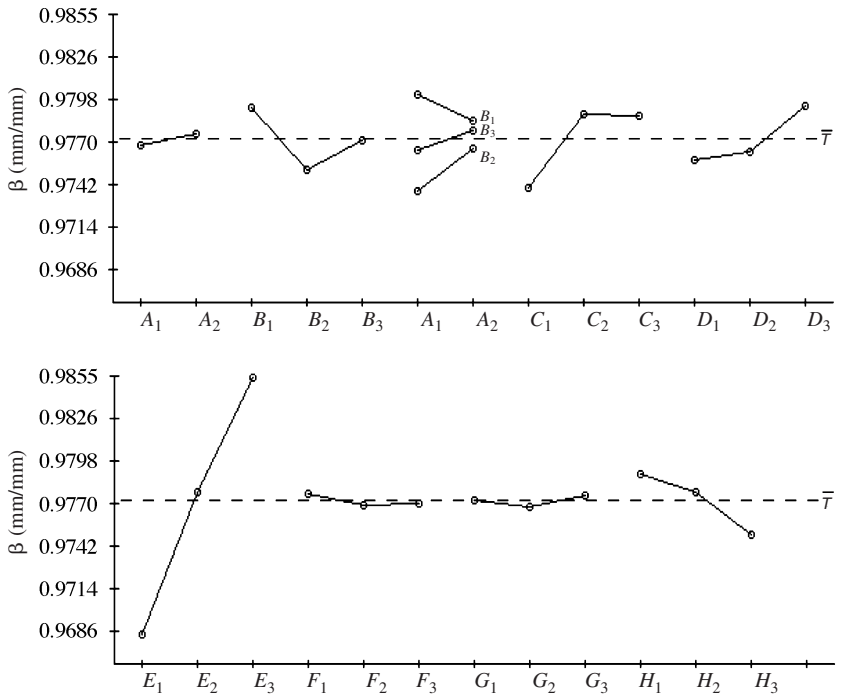

Figure 10
Control-factor-level average graphs for zero-point proportional sensitivity, β

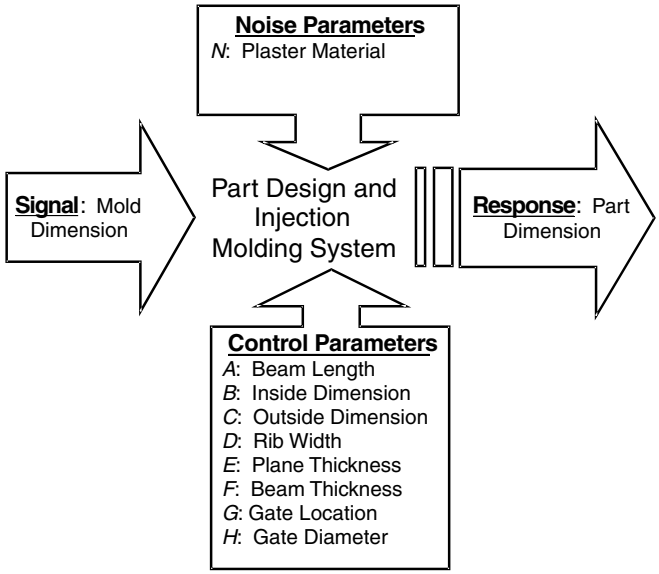

Figure 11
Parameter diagram for the all-axes dimension approach

Table 5
Factors and levels for the all-axes dimension approach

	Level											
Factor	**1**	**2**	**3**	**4**	**5**	**6**	**7**	**8**	**9**	**10**	**11**	**12**
Control factors												
A: beam length (mm)	10	12										
B: inside dimension (mm)	11.3	13.6	15.9									
C: outside dimension (mm)	3.38	5.68	7.98									
D: rib width (mm)	0	7	14									
E: plane thickness (mm)	0.6	0.88	1.25									
F: beam thickness (mm)	0.6	0.88	1.25									
G: gate location	*A*	*B*	*C*									
H: gate diameter (mm)	0.4	0.8	1.2									
Noise factors												
N: plastic material	*A*	*B*										
Signal factor												
M: mold dimension (mm)	0.48 2.94	0.60 3.10	0.65 6.42	0.80 20.0	0.90 35.1	1.07 55.4	1.20	1.35	1.80	2.04	2.20	2.65

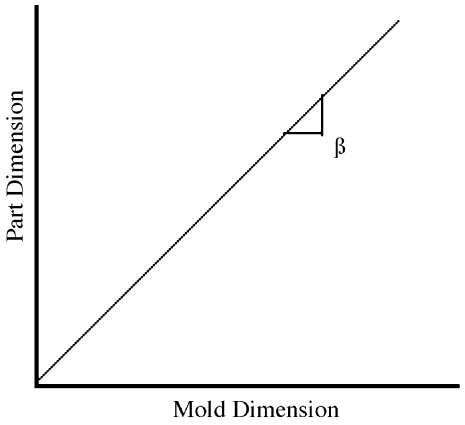

Figure 12
Ideal function for the all-axes dimension approach

Figure 11 presents the P diagram for this approach, and Table 5 the list of factors and levels.

Figure 12 shows the ideal function for this approach, and Figure 13 the finite-element node mesh associated with the signal factor levels (18). A slope of 1.00 would result in the mold and the part having identical dimensions.

Table 6 presents the orthogonal layout for this approach, along with the resulting zero-point proportional SN ratio and slope, β. Figures 14 and 15 present the zero-point SN and sensitivity (slope, β) control-factor-level average graphs for the dynamic all-axes dimension approach using the data in Table 6.

From these graphs, the best set of control factor levels is $A_2B_3C_2D_1E_3F_2G_1H_1$. Verification studies using this set were done and are reported along with the other approaches later.

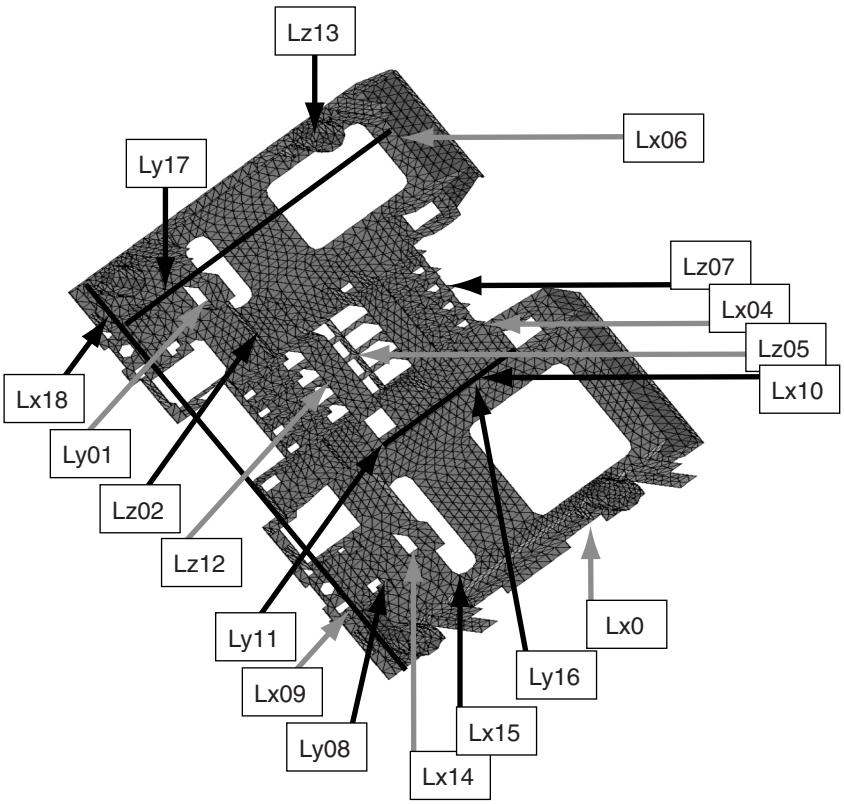

Figure 13
FE node mesh for the all-axes dimension approach

Table 6
Orthogonal layout and results for the all-axes approach

OA Row	Control Factor								Zero-Point SN	Slope, β
	A	*B*	*C*	*D*	*E*	*F*	*G*	*H*		
1	1	1	1	1	1	1	1	1	32.32	0.985
2	1	1	2	2	2	2	2	2	32.80	0.983
3	1	1	3	3	3	3	3	3	34.17	0.982
4	1	2	1	1	2	2	3	3	33.41	0.985
5	1	2	2	2	3	3	1	1	38.93	0.982
6	1	2	3	3	1	1	2	2	26.07	0.984
7	1	3	1	2	1	3	2	3	26.45	0.984
8	1	3	2	3	2	1	3	1	33.23	0.984
9	1	3	3	1	3	2	1	2	38.23	0.981
10	2	1	1	3	3	2	2	1	30.88	0.982
11	2	1	2	1	1	3	3	2	29.71	0.986
12	2	1	3	2	2	1	1	3	33.15	0.984
13	2	2	1	2	3	1	3	2	30.31	0.985
14	2	2	2	3	1	2	1	3	35.31	0.982
15	2	2	3	1	2	3	2	1	33.95	0.983
16	2	3	1	3	2	3	1	2	36.13	0.981
17	2	3	2	1	3	1	2	3	32.40	0.983
18	2	3	3	2	1	2	3	1	32.21	0.983

6. Verification and Comparison

Table 7 presents the predicted (assuming complete additivity in the L_{18} orthogonal array) and verified (computer simulation confirmed) SN and slope, β, values for the three approaches studied. In addition, a *Z*-axis deflection value was calculated using the computer simulation model for the three approaches.

Figures 16 and 17 show the computer simulation results of the *Z*-axis deflection calculated by using the Z_{max} minus Z_{min} deflection for material *A* added to Z_{max} minus Z_{min} for material *B*. Figure 16 is the same for approach 1 (smaller-the-best) and approach 2 (*Z*-axis position zero-point proportional) because these analyses resulted in the selection of the same optimum set of control parameter values. Figure 17 shows Approach 3 (all-axes dimension zero-point proportional). Figure 18 shows the worst-case image from the L_{18}.

7. Conclusions

1. All the computer simulation confirmed values are within the confidence interval predicted.
2. Approach 3, all-axes dimension zero-point proportional, results in the largest undesirable deflection on the electrical connector insulator part in the *Z*-axis.
3. Approach 1, smaller-the-best, and approach 2, *Z*-axis position zero-point proportional, results

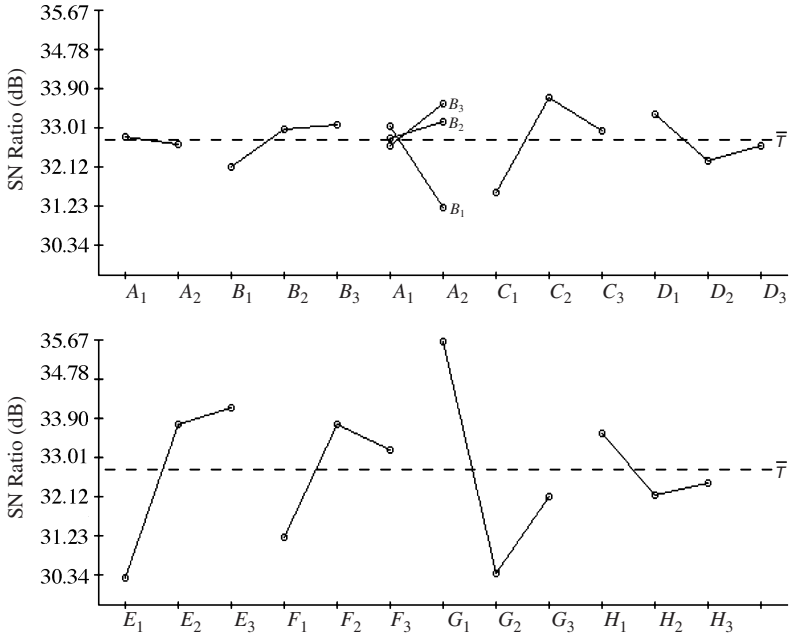

Figure 14
Control-factor-level average graphs

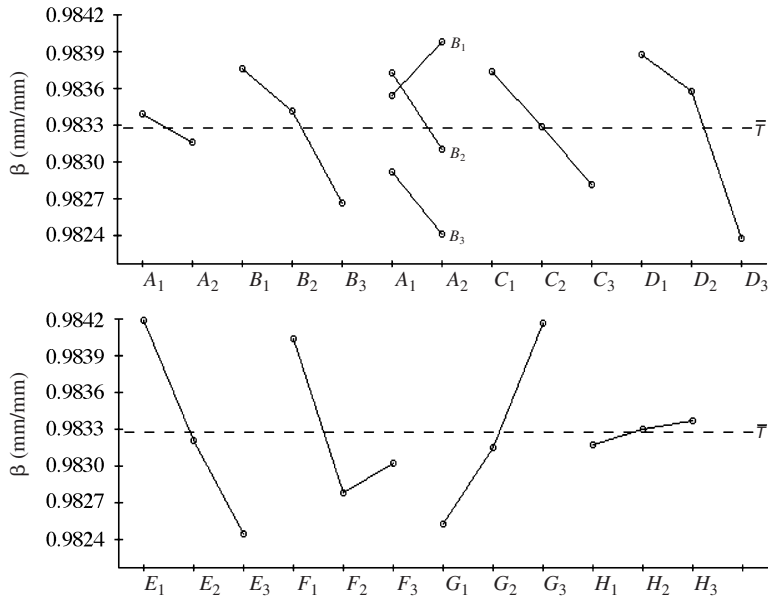

Figure 15
Control-factor-level average graphs zero-point slope, β, all-axes dimension

Table 7
Confirmation predictions and verification

Parameter Design Approach	Gate	Predicted SN (dB)	Predicted β	Verified (Simulation Confirmed) SN (dB)	Verified (Simulation Confirmed) β	Calculated Deflection from Mold Reference Z-Axis Delta (mm)
Smaller-the-best deflection on *z*-axis	G_1	18.99 ± 1.53	—	17.76	—	1.03
	G_2	18.28 ± 1.53	—	19.30	—	0.93
Zero-point proportional, *z*-axis position	G_1	18.80 ± 1.49	0.991 ± 0.004	17.86	0.986	1.03
	G_2	18.77 ± 1.49	0.990 ± 0.004	19.33	0.992	0.93
Zero-point proportional, all axes dimension	G_1	40.76 ± 4.42	0.981 ± 0.001	35.08	0.983	1.37
	G_2	35.50 ± 4.42	0.982 ± 0.001	31.61	0.984	1.17

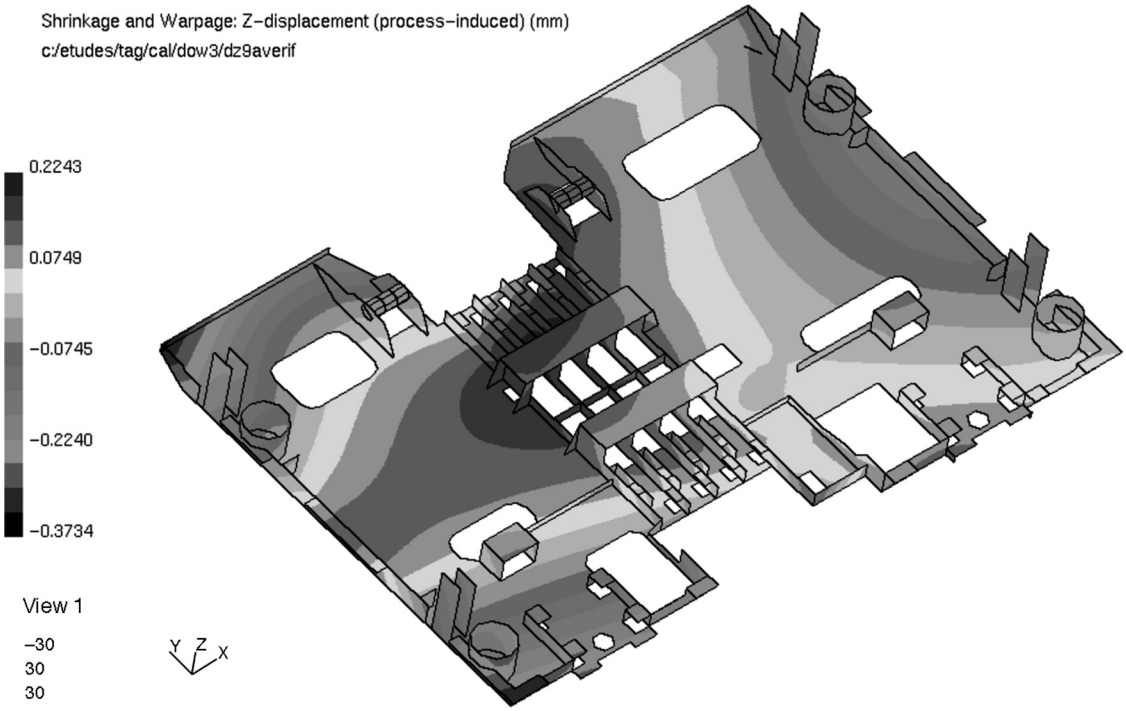

Figure 16
Verification of approach 1 (smaller-the-best *Z*-axis deflection) and approach 2 (*Z*-axis position zero-point proportional)

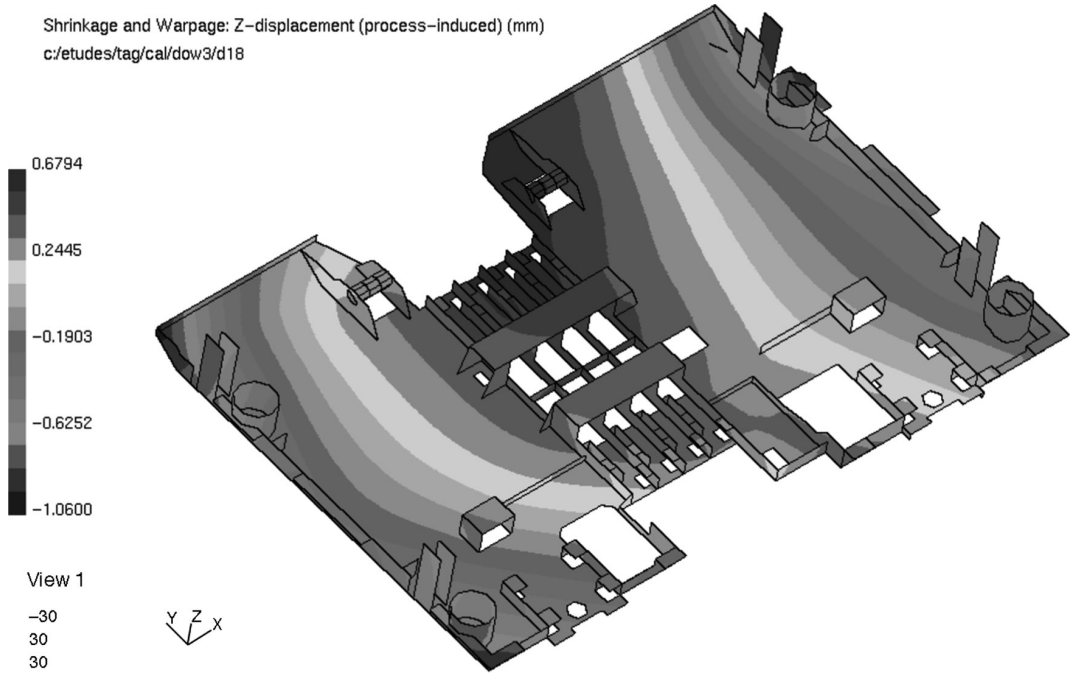

Figure 17
Verification of approach 3 (all-axes dimension zero-point proportional)

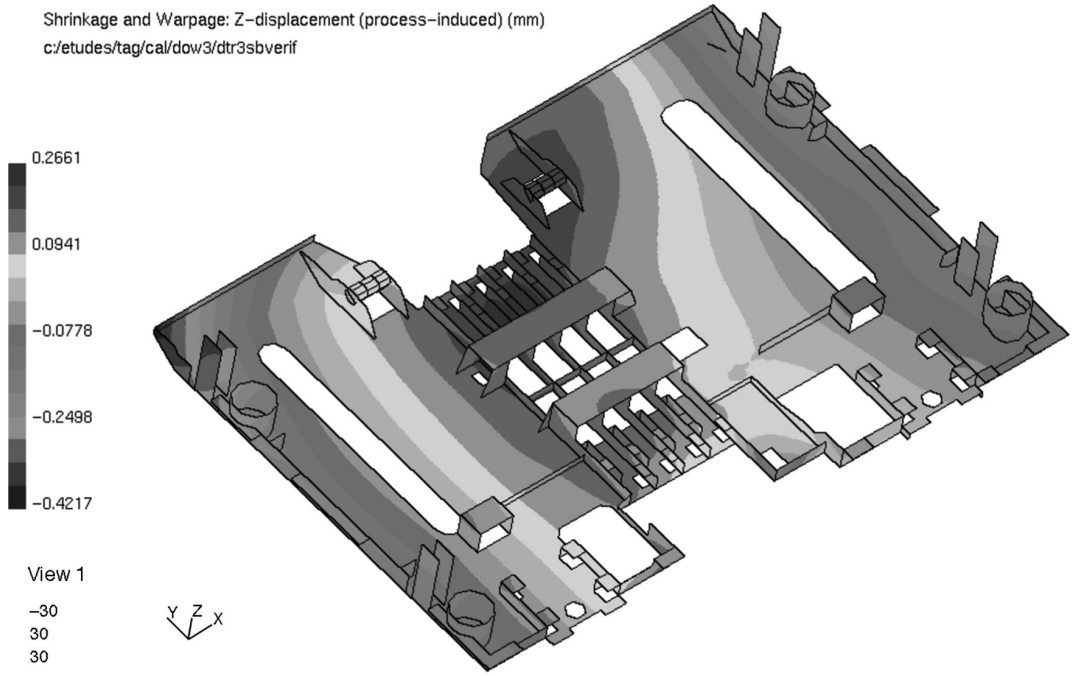

Figure 18
L_{18} worst case

are the same with the lowest associated *Z*-axis deflection.

4. Taguchi's parameter optimization methodology, coupled with computer simulation, provides a powerful tool for optimizing plastic part and tool design as well as the associated injection molding process. In addition, these coupled tools reduced product and process design time and tooling cost by eliminating the need to build prototypes with injection molding tools of various designs.
5. Applying the results of this study to the CCM02 MKII electrical connector contact housing part and tool resulted in less than 0.15 mm of *Z*-axis deformation for hardware produced using the optimum control parameter value set. This was less that the 1.0-mm average confirmed using the finite-element simulation software.

This case study is contributed by Marc Bland.